Ind. J. Pharm. Edu. Res., 2024; 58(4):1242-1254.
https://www.ijper.org

Original Article

Coumarin-1,2,3-Triazole Hybrids as Promising Antibacterial Agents: *In silico* Molecular Docking, ADMET and Molecular Dynamics Simulation Studies (Exploring *in silico* Antibacterial Potential of Coumarin-1,2,3-triazoles)

Krishna Narayan Mishra[1], Mayank Rashmi[2,3], Harish Chandra Upadhyay[1,*]

[1]Laboratory of Chemistry, Department of Applied Sciences, Rajkiya Engineering College (Affiliated with Dr. A.P.J. Abdul Kalam Technical University, Lucknow), Churk, Sonbhadra, Uttar Pradesh, INDIA.
[2]Center of Bioinformatics, IIDS, University of Allahabad, Prayagraj, Uttar Pradesh, INDIA.
[3]Division of Agricultural Bioinformatics, ICAR-Indian Agricultural Statistics Research Institute, New Delhi, INDIA.

ABSTRACT

Background: A lot of coumarin-1,2,3-triazole hybrids have been reported to show antibacterial activities, but most of them are unexplored in clinical studies. Herein, we wish to apply *in silico* docking, physiochemical predictions and molecular dynamics simulation studies on coumarin-1,2,3-triazole hybrids to explore their successful transformation in to broad spectrum antibacterial agent for clinical use. **Materials and Methods:** A library of 196 compounds with the coumarin-1,2,3-triazole motif showing antibacterial activity against various pathogenic bacteria was generated, and molecules were *in silico* screened for their binding affinities through molecular docking against six antibacterial targets Dihydropteroate synthase (PDB, ID:1TX2), Penicillin-binding protein-3 (PDB, ID:3OCN), DNA Gyrase-B24 (PDB, ID:6YD9), UDP-N-Acetylglucosamine enolpyruvyl transferase (PDB, ID:1UAE), Sortase A (PDB, ID:2MLM), and Dethiobiotin synthetase (PDB, ID:4WOP) using AutoDock Vina. On the basis of high docking score and suitable physiochemical and ADMET parameters hybrids 134, 143, 174, and 176 were subjected to 100 ns of Molecular Dynamics (MD) on GROMACS to investigate the protein-ligand complex's stability. **Results:** All the coumarin-1,2,3-triazole hybrids docked well with the target antibacterial protein and most of them exhibited higher binding affinity than the co-crystallized ligands of the respective proteins. MD simulation results in terms of Root Mean Square Deviation (RMSD), Root Mean Square Fluctuation (RMSF), Radius of gyration (Rg) and distribution of hydrogen bonds were in complete agreement of docking scores indicating for stable ligand-target bonding. **Conclusion:** This study provides strong evidence for coumarin-1,2,3-triazole hybrids to be excellent antibacterial agents effective on both Gram-positive and Gram-negative pathogenic strains and hybrid 176 may be considered the best out of all.

Keywords: Coumarin-1,2,3-triazoles, antibacterial, docking, Molecular Dynamics, ADMET, Drug resistance.

Correspondence:
Dr. Harish Chandra Upadhyay
Department of Applied Sciences,
Rajkiya Engineering College, Churk,
Sonbhadra-231206, Uttar Pradesh, INDIA.
Email: harishcu@gmail.com

Received: 19-10-2023;
Revised: 07-12-2023;
Accepted: 20-08-2024.

INTRODUCTION

The process of discovering new drugs entails choosing potential candidates, synthesizing, characterizing, validating, optimizing, screening, and conducting assays to determine therapeutic efficacy.[1] Drug development involves converting the end-product of the discovery phase into a product approved for marketing by the appropriate regulatory authorities.[1,2] The entire drug discovery and development process is a multidisciplinary, time-consuming, costly (yet rewarding), and often unsuccessful process.[3,4] Many rational factors are responsible for drug development failures, such as patient stratification, animal model translational failures, misinterpretations of biological mechanisms and disease biomarkers, and non-reproducibility of preliminary data.[5] Safety and efficacy are the major issues in the failure of investigational drugs in late-stage clinical development. In the time frame of 1998-2008, among 640 novel therapeutics, only 230 (36%) were approved by the US Food and Drug Administration (FDA), of which about 57% failed because of efficacy and 17% because of safety concerns.[3,5]

In silico drug design, also known as Computer-Aided Drug Design (CADD), is becoming a mainstream approach to drug

DOI: 10.5530/ijper.58.4.137

discovery and development due to advances in computational power and sophistication in hardware and software, the identification of molecular targets, and an expanding database of target protein structures that are publicly available.[6,7] The Pharmacokinetic (PK) properties, viz., Absorption, Distribution, Metabolism, Excretion, and Toxicity (ADMET) profile, of the leads can be accurately and precisely predicted by using CADD to avoid safety issues in clinical trials.[8] Structure-based drug designs has achieved success with molecular docking, which predicts the binding affinity of the ligand with the target protein by computing the energy of interaction between the ligand and the protein.[9,10] The ligand-protein docking process allows for the screening of large chemical libraries to identify potential hits.[11] The stability of protein-ligand complexes and the mechanism of ligand binding can be studied by simulating the mobility of atoms in the system over time, which enables the prediction of the conformational changes that take place during protein-ligand binding.[12] When combined, molecular docking and molecular dynamics modelling can yield important information on how tiny compounds interact with target proteins, which can help in the discovery of novel therapeutics. Recent research has shown how useful these methods are for finding new treatments for a range of illnesses, accelerating up the drug the development process and cutting expenses and time.[13,14]

Modern pharma has greatly benefited from the molecules of natural sources.[15,16] In reality, natural products or their derivatives make up more than half of the licensed drugs on the market today.[17-20] In harmony with nature, natural chemical entities are regarded as safe in clinical applications.[21,22] Coumarins (2H-1-Benzopyran-2-one) are the phenolic ingredient that occurs naturally in a broad variety of plants, bacteria, and fungi.[23,24] The diverse class of naturally occurring pharmacophores known as coumarins displays a wide range of biological activities, including anti-inflammatory, antioxidant, antinociceptive, hepatoprotective, antithrombotic, antiviral, antimicrobial, antituberculosis, anticancer, antidepressant, antihyperlipidemic, anti-Alzheimer, anticholinesterase, and antiviral properties.[23-25] Natural and synthetic compounds with coumarin scaffolds are widely used in clinical applications. Nevertheless, numerous Nitrogen based heterocyclic secondary compounds from algae, fungi, and other species have been shown to have a variety of pharmacological merits, including anti-cancer, anti-HIV, anti-malarial, anti-tubercular, anti-microbial, and antidiabetic properties.[26,27] The versatility of nitrogen's interactions with biological targets has made both naturally occurring and synthetic nitrogen-based heterocyclic molecules appealing to medicinal scientists.[27,28] On the other hand, the emergence and perpetuation of drug resistance in pathogenic microbes pose a serious health risk on a global scale.[29,30] The worldwide loss of life from antibiotic resistance reached 1.27 million in 2019 and is projected to reach 10 million yearly deaths by 2050.[31,32] The pipeline of available antibiotics is not adequate to satisfy projected and existing therapeutic needs.[33] When compared to drugs that work on multiple targets, which may have better efficacy, lower resistance, and fewer side effects, it has been noted that single-target drugs frequently cause resistance and are associated with side effects.[34,35] As a result, the most widely used "one molecule, one target" strategy in drug discovery is now being changed to "one molecule, multiple targets" by designing hybrid molecules.[34,36]

Numerous efforts have been made by synthetic chemists to develop hybrid molecules of coumarin and 1,2,3-triazole, the biologically active pharmacophores.[37,38] Few of the reviews on the improvements and applications of coumarin-1,2,3-triazole hybrid compounds as possible bioactive leads have been encompassed, which report mostly *in vitro* antibacterial and anticancer activities.[37,38] In order to have a deep understanding of the antimicrobial potential of coumarin-1,2,3-triazole hybrids, the current study has been designed for the investigation of *in silico* binding affinity with antimicrobial targets by molecular docking and molecular dynamics simulations. A total of 196 coumarin-1,2,3-triazole hybrids with preliminary antibacterial activity against various pathogenic bacteria reported in our earlier review.[38] Were *in silico* examined for their binding affinities through molecular docking against six antibacterial targets. The top hits were examined for their suitability on physiochemical and ADMET parameters for an oral drug. Further, to investigate the protein-ligand complex's stability, select molecules were subjected to molecular dynamics simulation studies.

MATERIALS AND METHODS

Data collection and Ligand Preparation

The compounds exhibiting antibacterial action against different pathogenic microorganisms and possessing the coumarin-1,2,3-triazole motif were obtained from a publication.[38] A library of 196 compounds was generated by drawing the 2D structures on ChemDraw-v22. The structures were transformed into 3D and geometry was cleaned using ChemBioDraw-Ultra-v22.0 (http://www.cambridgesoft.com). Energy minimization was performed with MM2 molecular mechanics parameters until achieving the lowest stable energy (<0.001 kcal/mol). Later they were saved as mol files. The co-crystallised ligands of the respective proteins retrieved from PDB were separated and used as positive control. The SMILES of all the ligands for physiochemical and ADMET predictions were generated from mol files on OPENBABEL online platform (http://www.cheminfo.org/Chemistry/Cheminformatics/FormatConverter/index.html).

Docking studies

Target preparation

The experimentally reported six target proteins of three gram-positive and three Gram-negative bacteria were selected

Table 1: The antibacterial targets.

Sl. No.	Target name	Organism	Pathway	PDB ID	References
1	Penicillin-binding protein 3	*Pseudomonas aeruginosa,* Gram-negative, rod shaped.	Peptidoglycan synthesis	3OCN	55
2	DNA Gyrase B24	*Escherichia coli* K-12, Gram-negative, rod shaped.	DNA synthesis	6YD9	56
3	UDP-N-Acetylglucosamine Enolpyruvyl Transferase	*Escherichia coli,* Gram-negative, rod shaped.	Peptidoglycan pathway	1UAE	57
4	Dihydropteroate synthase	*Bacillus anthracis,* Gram-positive, rod shaped.	Folate pathway	1TX2	58
5	Sortase A	*Staphylococcus aureus* CA-347, Gram-positive, spherically shaped.	Sortase pathway	2MLM	59
6	Dethiobiotin synthetase	*Mycobacterium tuberculosis* H37Ra, Gram-positive, rod shaped.	Biotin synthesis pathway	4WOP	60

to analyse the inhibitory action of hybrid compounds (Table 1). Three dimensional (3-D) crystallographic structures of target proteins were downloaded from Protein Data Bank (PDB, www.rcsb.org). The targets Dihydropteroate synthase (PDB, ID:1TX2), Penicillin-binding protein-3 (PDB, ID:3OCN), DNA Gyrase-B24 (PDB, ID:6YD9), UDP-N-Acetylglucosamine-enolpyruvyl transferase (PDB, ID:1UAE), Sortase A (PDB, ID:2MLM), and Dethiobiotin synthetase (PDB, ID:4WOP) were prepared using AutoDockTools4 by removing hetero atoms and adding missing hydrogen atoms as well as Gasteiger charges then file save as PDBQT format which is acceptable by Autodock-Vina.[39]

Structure based virtual screening

The Autodock-Vina was used for the structure based virtual screening by docking of the ligands against all selected six targets. The active site residues and coordinates of target proteins were identified by the information provided in PDB. The grid box in Autodock-Vina for each protein were generated targeting the active site of the protein and the parameters viz. active site centre coordinates, grid box size and active site residues. The exhaustiveness was kept 8 and all other parameters were kept default for screening by the software.[40,41] Best out of ten configurations for each protein-ligand complex were considered and Excel files of docking score results were also produced for the purpose of manual comparative analysis at the end of the experiment. The protein-ligand complexes along with the molecular interaction were all visualized using AutoDock.

Computational pharmacokinetics analysis

The SwissADME (http://www.swissadme.ch/) free web tool was used for evaluating the pharmacokinetics, drug-likeness and medicinal chemistry friendliness of coumarin-triazole hybrid molecules.[42] Various physicochemical parameters such as Molecular weight, Log P, hydrogen bond donor, hydrogen bond acceptor, total polar surface area, and number of rotatable bonds were estimated and checked for their familiarity with Lipinski's rule of five.[43,44] The pkCSM server (http://biosig.unimelb.edu.au/pkcsm/prediction) was used to predict the ADMET property of selected coumarin-1,2,3-triazole hybrid molecules.[45] Various parameters for Absorption (viz. Caco2 permeability, human intestinal absorption, Skin Permeability), distribution (viz. human VDss, BBB permeability, CNS permeability), metabolism (viz. effect on cytochromes P450), excretion (viz. Total Clearance, Renal OCT2 substrate) and toxicity (viz. AMES toxicity, Oral Rat Acute Toxicity (LD50), Oral Rat Chronic Toxicity (LOAEL), Hepatotoxicity, Skin Sensitisation) were taken in to account.

Molecular Dynamics Simulation studies

Four compounds, numbered 134, 143, 174, and 176, were chosen for MD modelling based on ADMET, physicochemical characteristics, and binding scores. GROMACS 2020 along with the CHARMM 36m force field were used to perform the MD simulation studies.[46,47] Utilising the CHARMM-GUI Web Server, the complexes of the four compounds were utilised to generate the system input data.[48] The complexes were placed in a cuboidal box after being solvated utilising the TIP3P water model.[49] The entire system was neutralized using the Monte-Carlo ion placement approach by introducing Na^+ and Cl^- ions.[50] The constructed systems were put through a 50000-step most steep energy reduction process.[51] Then, in a temperature of 310.15 K, a 1 ns equilibration step was carried out via Nose-Hoover temperature coupling employing constant Number, Volume, and Temperature (NVT).[52] The system went through a simulation of isobaric-isothermal (NPT) generation that lasted 100 ns at periodic boundary conditions and used the Parrinello-Rahman pressure coupled at 1 atm pressure. The obtained simulation path was then quantitatively analysed by computing various parameters such as the Radius of gyration (Rg), Root-Mean-Square Fluctuation (RMSF), Root-Mean-Square Deviation (RMSD) and hydrogen bond distribution using the gmx rms, gmx rmsf, gmx gyrate, and gmx H-bond functionalities, which are all available in GROMACS.[53]

Table 2: Docking Scores (Binding Energies) of select ligands with antibacterial target proteins.

1TX2		6YD9		4WOP		3OCN		2MLM		1UAE	
Comp.	B.E.	Comp.	B.E.	Comp.	B.E.	Comp.	B.E.	Comp.	B.E.	Comp.	B.E.
176	-12.543	176	-10.677	185	-11.976	143	-11.36	175	-11.606	175	-14.097
174	-12.031	175	-10.312	176	-11.628	178	-10.887	176	-11.415	174	-13.102
175	-11.522	171	-10.232	175	-11.619	175	-10.872	145	-11.259	173	-13.065
145	-11.02	177	-10.006	182	-11.168	134	-10.837	143	-11.011	145	-12.966
143	-10.922	55	-9.843	145	-11.042	144	-10.66	177	-10.877	134	-12.917
171	-10.733	166	-9.726	171	-11.023	176	-10.635	185	-10.873	167	-12.847
168	-10.708	174	-9.693	174	-10.867	171	-10.629	168	-10.848	168	-12.747
170	-10.607	178	-9.596	168	-10.7	174	-10.499	174	-10.739	176	-12.743
172	-10.406	173	-9.591	178	-10.636	177	-10.38	134	-10.686	171	-12.716
167	-10.278	168	-9.566	183	-10.625	180	-10.323	133	-10.584	172	-12.585
144	-10.264	101	-9.45	143	-10.552	185	-10.18	184	-10.57	133	-12.537
181	-10.204	167	-9.44	167	-10.525	167	-10.045	173	-10.564	184	-12.315
184	-9.958	134	-9.275	172	-10.489	182	-10.013	167	-10.517	151	-12.04
17	-9.852	130	-9.219	173	-10.481	172	-9.983	171	-10.462	18	-11.998
134	-9.83	169	-9.217	177	-10.468	165	-9.951	181	-10.458	182	-11.991
182	-9.64	133	-9.1	144	-10.439	146	-9.919	144	-10.208	157	-11.882
164	-9.52	149	-9.092	116	-10.423	186	-9.875	165	-10.146	165	-11.795
19	-9.493	143	-9.074	113	-10.301	179	-9.808	172	-10.041	170	-11.756
185	-9.423	128	-9.007	110	-10.262	151	-9.797	166	-10.04	169	-11.681
169	-9.338	141	-8.961	180	-10.189	104	-9.791	180	-10.015	143	-11.665
180	-9.329	142	-8.936	114	-10.179	125	-9.758	141	-9.932	21	-11.606
96	-9.318	170	-8.906	117	-10.163	191	-9.733	182	-9.92	128	-11.584
109	-9.313	179	-8.87	111	-10.134	132	-9.707	183	-9.849	164	-11.554
103	-9.286	102	-8.868	129	-10.13	170	-9.647	117	-9.823	192	-11.452
130	-9.255	192	-8.815	133	-10.127	15	-9.642	116	-9.822	22	-11.426
55	-9.246	189	-8.814	119	-9.992	154	-9.632	132	-9.802	125	-11.329
166	-9.241	131	-8.781	124	-9.976	141	-9.575	192	-9.781	156	-11.299
114	-9.239	110	-8.762	141	-9.966	156	-9.536	111	-9.779	129	-11.299
38	-9.238	47	-8.71	120	-9.965	190	-9.491	142	-9.776	43	-11.276
178	-9.224	151	-8.679	128	-9.963	183	-9.466	125	-9.758	166	-11.256
179	-9.186	116	-8.664	112	-9.911	127	-9.463	178	-9.742	144	-11.254
160	-9.183	111	-8.646	115	-9.906	124	-9.46	110	-9.733	185	-11.235
125	-9.136	37	-8.635	184	-9.89	135	-9.409	102	-9.732	132	-11.235
146	-9.125	182	-8.598	109	-9.871	96	-9.358	170	-9.712	55	-11.232
129	-9.124	124	-8.588	151	-9.867	188	-9.311	112	-9.708	130	-11.204
18	-9.075	117	-8.583	166	-9.849	166	-9.308	135	-9.7	150	-11.2
128	-9.023	38	-8.571	147	-9.844	169	-9.282	128	-9.682	126	-11.19
100	-8.983	120	-8.552	136	-9.815	116	-9.253	113	-9.677	44	-11.18
165	-8.95	135	-8.54	55	-9.795	129	-9.24	114	-9.669	135	-11.173
22	-8.946	165	-8.519	169	-9.77	113	-9.232	55	-9.661	142	-11.165
173	-8.905	113	-8.498	191	-9.765	128	-9.206	109	-9.64	191	-11.156

1TX2		6YD9		4WOP		3OCN		2MLM		1UAE	
Comp.	B.E.	Comp.	B.E.	Comp.	B.E.	Comp.	B.E.	Comp.	B.E.	Comp.	B.E.
13	-8.903	20	-8.483	118	-9.692	117	-9.194	115	-9.635	97	-11.155
99	-8.857	109	-8.479	134	-9.69	119	-9.188	21	-9.619	146	-11.145
122	-8.852	119	-8.475	130	-9.673	55	-9.181	129	-9.565	163	-11.102
189	-8.84	129	-8.424	125	-9.565	110	-9.168	120	-9.538	136	-11.075
CCL1	-5.882	CCL2	-7.344	CCL3	-8.3	CCL4	-7.268	CCL5	-7.778	CCL6	-8.164
DAP	-6.186	GATI	-7.055	-	-	CEF	-7.392	-	-	FOS	-4.616

Compd.: Compound, B.E.: Binding Energy (kcal/mol), CCL1: 6-Methylamino-5-nitroisocytosine, CCL2: N-[6-(3-azanylpropanoylamino)-1,3-benzothiazol-2-yl]-3,4-bis(chloranyl)-5-methyl-1H-pyrrole-2-carboxamide, CCL3: Cytidine-5'-triphosphate, CCL4: 1-({(2R)-2-[(1R)-1-{[(2Z)-2-(2-amino-1,3-thiazol-4-yl)-2-{[(2-carboxypropan-2-yl)oxy]imino}acetyl]amino}-2-oxoethyl]-4-carboxy-3,6-dihydro-2H-1,3-thiazin-5-yl}methyl)pyridinium, CCL5: N-{2-oxo-2-[(3s,5s,7s)-tricyclo[3.3.1.1~3,7~]dec-1-ylamino]ethyl}-2-sulfanylbenzamide, CCL6: Uridine-diphosphate-N-acetylglucosamine, DAP: Dapsone, GATI: Gatifloxacin, CEF: Cefixime, FOS: Fosfomycin

RESULTS AND DISCUSSION

Docking Studies

Molecular docking is a powerful computational technique that plays a pivotal role in modern drug discovery for the prediction and analysis of the binding modes between a small molecule (a ligand) and its target protein (a receptor). The mechanism by which antibiotics cause bacterial cell death is a complicated process that involves changes to the affected bacterium at the biochemical, molecular, and ultrastructural levels as well as a physical interaction between a drug molecule and its specific target in bacteria. Most of the today's antibiotics inhibit DNA, RNA, cell wall or protein synthesis in bacteria. The antibacterial target proteins are those which are reported to be involved in various synthetic pathways crucial for the bacterial life cycle.[54] In view of increasing resistant strains of bacteria, it will be better to choose a molecule simultaneously inhibiting more than one type of metabolic pathways.[16,35,38] In an effort to find alternative broad-spectrum antibacterial agents, six antibacterial target proteins-three belonging to gram-negative and another three to gram-positive bacterial strains-were selected for docking with coumarin-1,2,3-triazole derivatives. The details of all the six target proteins are presented in Table 1.

Autodock Vina employs a grid-based search algorithm to explore the conformational space and predict the optimal binding pose of the ligand within the receptor's active site.[40,41] Grid centre coordinates and active site residues of selected six targets are depicted in Table S1 of supporting information. The docking scores in terms of binding energies of top 45 docked ligands with antibacterial target proteins have been presented in Table 2, while the docking scores of all the ligands with target proteins is provided in Table S2 of supporting information.

All the coumarin-1,2,3-triazole hybrids docked well with the target antibacterial proteins (Table 3). Out of 196 docked compounds, except compound 67, all showed higher binding affinity than the co-crystallized ligand (CCL1) with the target protein 1TX2. The compounds 176, 174, 175, and 145 showed almost double or even more binding energy than CCL1. Interestingly, 192 out of 196 compounds showed higher binding affinity than the reference antibiotic Dapsone (DAP) against 1TX2. Similar results were obtained against other antibacterial targets, where the majority of the hybrids exhibited higher binding affinity than the co-crystallized ligands of the respective proteins. The interaction of Amino acid residues of target proteins with selected ligands is mentioned in Table 3.

The interactions of selected compounds with the 6YD9 target are shown in Figure 1. It is clearly seen that the compounds interacted at the same site of target as the reference compound, a co-crystallized ligand. The CCL2 interacted with the -7.344 binding affinity, and the residues are HIS83, ILE94, ALA100, GLY101, GLY102, and ARG136. Compound 134 showed interaction with HIS83, ILE94, GLY101, GLY102, PHE104, and ASP105, and the binding affinity is -9.275. The interacting residues with compound 143 are PRO79, HIS83, ALA90, ILE94, GLY101, GLY102, ASP105, SER108, and TYR109 with -9.074 binding affinity. Compound 174 interacted with GLU50, ILE78, PRO79, GLU85, ALA90, ILE94, ALA100, GLY101, TYR109, and THR165 at -9.693 binding affinity. The compound 176 interacted with the lowest binding affinity of -10.677 with residues PRO79, HIS83, ALA90, ILE94, GLY102, PHE104, ASP105, and ASN107 of the target 6YD9.

Computational pharmacokinetics

The physiochemical characteristics of a drug candidate, such as its solubility, lipophilicity, and molecular weight, are crucial for estimating a drug's solubility and likelihood of being effective during the early stages of drug discovery.[61] ADME (absorption, distribution, metabolism, and excretion) properties are the key determinants of a drug's efficacy and safety.[61,62] Poor absorption, rapid metabolism, or poor excretion can lead to poor pharmacokinetics and low efficacy, while poor metabolism or excretion can lead to toxicity. It is noticeable that, after entering clinical research, nine out of ten drug candidates are likely to fail during phase I, phase II, and phase III clinical trials and the drug approval process. Lack of clinical efficacy, intolerable toxicity, and poor drug-like qualities are among the top pharmacological

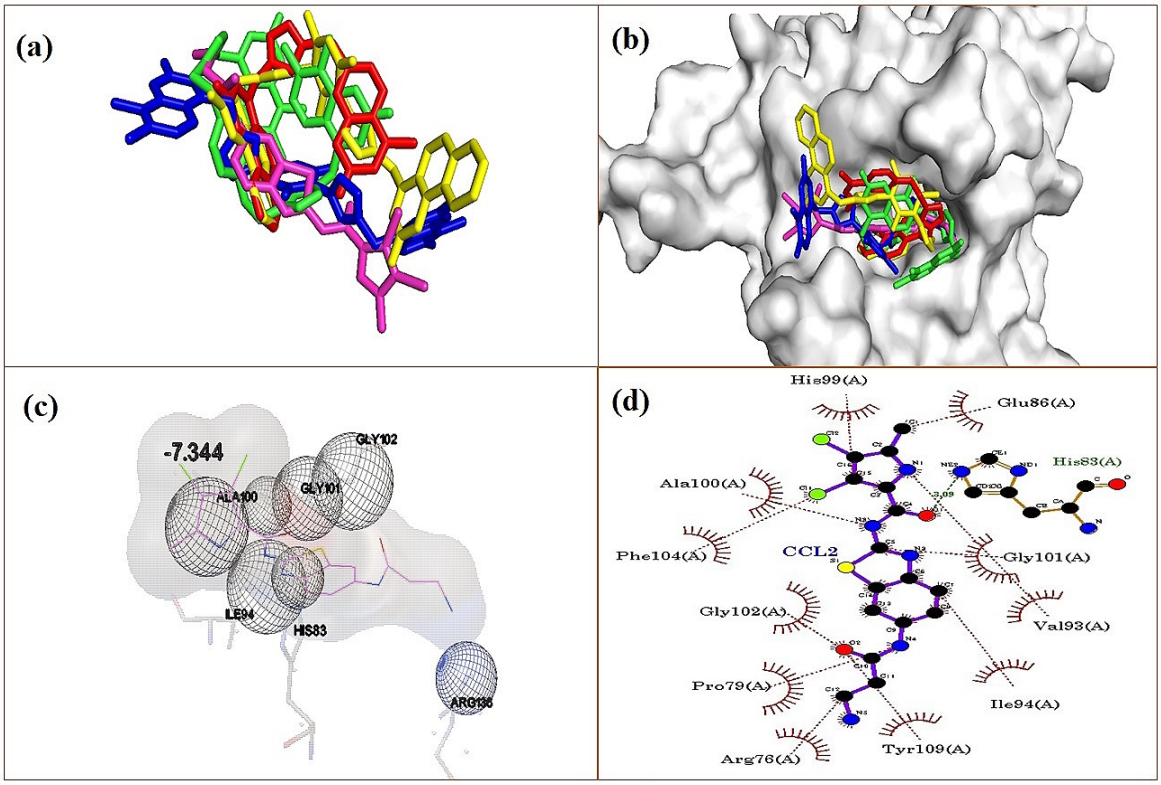
(a)
(b)
(c)
-7.344
GLY102
GLY101
ALA100
ILE94
HIS83
ARG136
(d)
His99(A)
Glu86(A)
His83(A)
Ala100(A)
Phe104(A)
CCL2
Gly101(A)
Gly102(A)
Val93(A)
Pro79(A)
Ile94(A)
Arg76(A)
Tyr109(A)

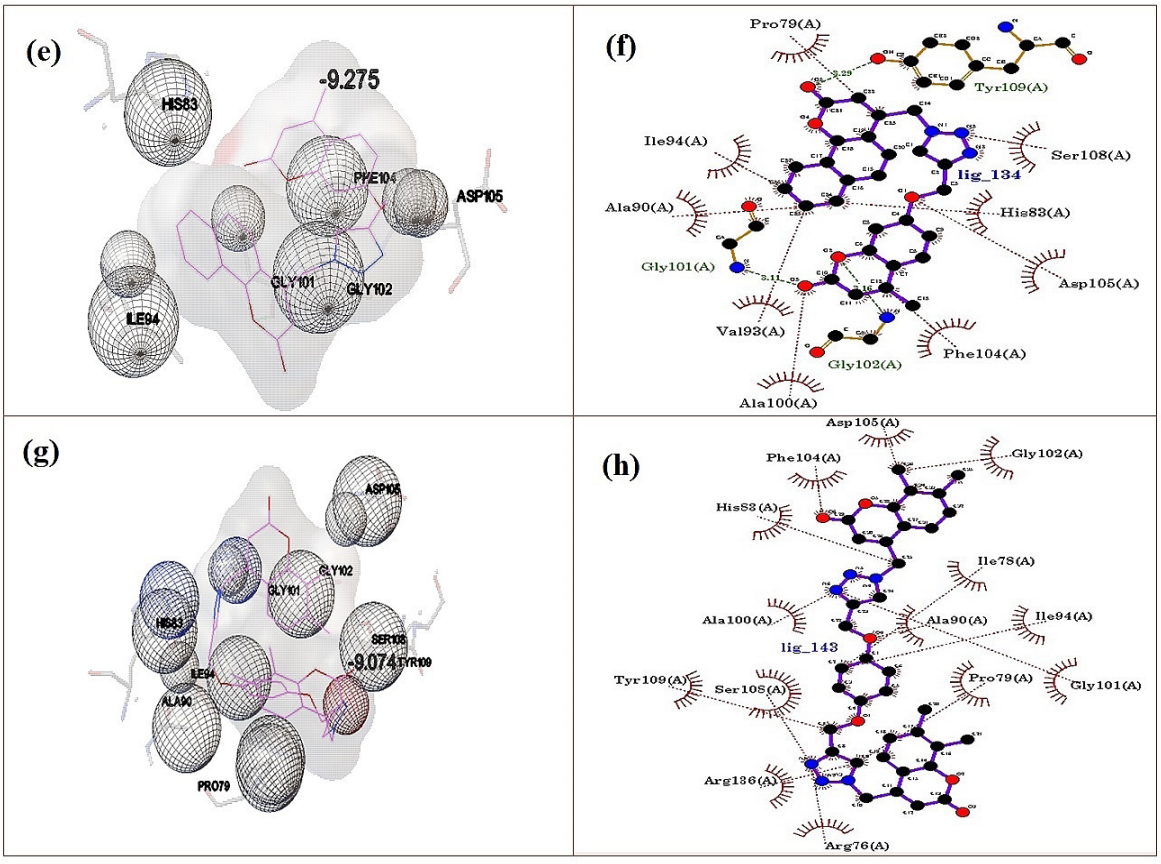
(e)
-9.275
HIS83
PHE104
ASP105
GLY101
GLY102
ILE94
(f)
Pro79(A)
Tyr109(A)
Ile94(A)
Ser108(A)
lig_134
Ala90(A)
His83(A)
Gly101(A)
Asp105(A)
Val93(A)
Phe104(A)
Gly102(A)
Ala100(A)
(g)
ASP105
GLY102
GLY101
HIS83
SER108
-9.074
TYR109
ILE94
ALA90
PRO79
(h)
Asp105(A)
Phe104(A)
Gly102(A)
His83(A)
Ile78(A)
Ala100(A)
Ala90(A)
Ile94(A)
lig_143
Tyr109(A)
Ser108(A)
Pro79(A)
Gly101(A)
Arg136(A)
Arg76(A)

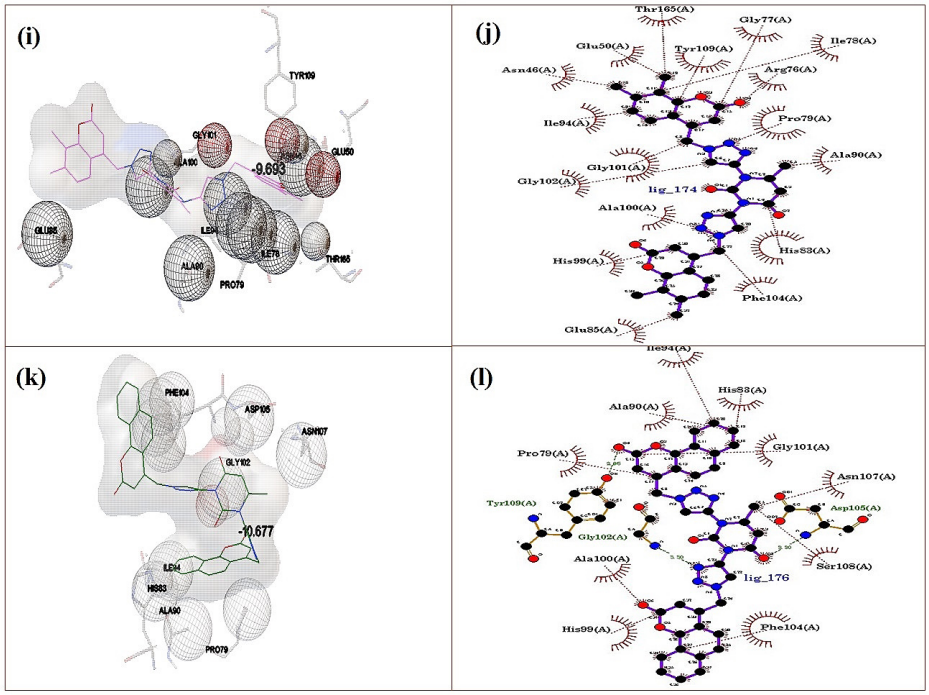

Figure 1: Docking confirmation, interacted residues and binding affinity score of 6YD9 with selected ligands. Aligned confirmation of ligands: reference/CCL2 (magenta), 134 (red), 143 (green), 174 (blue), 176 (yellow) are presented in Figure 1a-b; 2D and 3D representation of ligands interactions with 6YD9: reference/CCL2 (Figure 1c-d), 134 (Figure 1e-f), 143 (Figure 1g-h), 174 (Figure 1i-j) and, 176 (Figure 1k-l) with 6YD9 residues.

factors that contribute most often to drug failure.[63] Issues with ADME account for about 40% of all medication failures.[62] Therefore, physiochemical and ADME prediction are important aspects of drug discovery and by predicting and optimizing these properties, drug discovery researchers can increase the chances of success in later stages of development.[62,64] Seventy compounds from the top 30 hits of all six target proteins in docking studies were evaluated for their physiochemical parameters on the SwissADME online tool[42,65] The valued physiochemical parameters of the selected coumarin-1,2,3-triazole hybrids are presented in Table 4 (see Table S3 for all compounds). Further, the pkCSM server was used to predict various pharmacokinetic parameters of ADMET. The results of selected hybrid molecules with favorable physiochemical characteristics are tabulated in Table 5 (also refer to Table S4).

Any molecule with an intestinal absorption rate of less than 30% is regarded as having low absorbability.[66,67] Out of seventy compounds under investigation, only eight showed 68-88% intestinal absorption, while the rest showed 90-100% intestinal absorption. For optimal drug penetration and permeation, the physiology of the skin barrier must be better understood.[68,69] At the pkCSM server, a molecule with logKp >-2.5 is considered relatively less permeable through skin [67]. All the compounds showed skin permeability in the range of -2.731 to -2.749, which is an adjustable range. Caco-2 cells are a commonly used *in vitro* model of orally administered drugs for predicting drug absorption in the human intestinal epithelium. If any compound predicted by the pkCSM predictive model shows log P in 10^{-6} cm/s >0.90, it is considered high Caco-2 permeable.[70] Out of seventy, only thirty-four compounds passed the criteria of Caco-2 permeability. The Blood-Brain Barrier (BBB) is a selective barrier that restricts the entry of many drugs into the Central Nervous System (CNS).[71] In order to prevent potential psychiatric side effects, pharmaceuticals that are intended to treat other parts of the body should not cross the BBB.[72,73] All the tested compounds showed BBB in the range of -0.591 to -2.800, showing non-permeability to the CNS. A higher theoretical volume of distribution (VDss) indicates that the drug is more widely distributed in tissue than plasma. The VDss in log VDss<-0.15 (VDss<0.71 L/kg) is regarded as a low volume of distribution, and log VDss>0.45 (VDss>2.81 L/kg) is considered a high volume of distribution, based on the pkCSM prediction model. All the tested coumarin triazole hybrids exhibited a low volume of distribution, indicating their potential ability to show a pharmacological effect. The pkCSM prediction model suggests that molecules with CNS permeability (logPS) values greater than -2 are thought to penetrate the CNS, while those with logPS values less than -3 are unable to penetrate the CNS.[45,67] Only ten compounds exhibited logPS values greater than -2, hence predicted as able to penetrate the CNS, while the rest pass the criteria of a non-CNS drug. Cytochrome P450 (CYP) enzymes

Table 3: Interaction of Amino acid residues of target proteins with selected ligands.

Protein ID	Compound 134		Compound 143		Compound 174		Compounds 176		Reference Compound/CCL	
	B.A.	Int. Res.	B.A.	Int. Res.	B.A.	Int. Res.	B.A.	Int. Res.	B.A.	Int. Res.
6YD9	-9.275	HIS83, ILE94, GLY101, GLY102, PHE104, ASP105	-9.074	PRO79, HIS83, ALA90, ILE94, GLY101, GLY102, ASP105, SER108, TYR109	-9.693	GLU50, ILE78, PRO79, GLU85, ALA90, ILE94, ALA100, GLY101, TYR109, THR165	-10.677	PRO79, HIS83, ALA90, ILE94, GLY102, PHE104, ASP105, ASN107	-7.344	HIS83, ILE94, ALA10, GLY10, GLY10, ARG136
3OCN	-10.837	SER279, TYR313, VAL318, SER334, TYR392, TYR394, SER470, GLY471, THR472, ARG474, LYS475	-11.36	SER279, TYR302, ASN336, SER334, TYR394, GLY471, ARG474, LYS475, VAL476, ASN486, TYR488, LEU521,	-10.499	VAL456, PHE457, ARG458, THR472, ARG474, ASN486, TYR488, LEU521	-10.635	VAL318, VAL456, PHE457, ARG458, THR472, ARG474, ASN486, TYR488, VAL522	-7.268	VAL31, SER334, VAL45, LYS469, THR47, TYR48, LEU521
1UAE	-12.917	ARG91, ARG120, LYS160, VAL163, GLY164, PRO298, THR304, VAL327, PHE328	-11.005	ARG91, ARG120, PRO121, LYS160, VAL163, GLY164, THR304, VAL327, PHE328, GLU329, PHE332, ASN350	-13.102	ARG91, TRP95, ARG120, PRO121, HIS125, LYS160, VAL163, GLY164, ARG232, VAL327,	-12.743	ARG120, PRO121, LYS160, SER162, VAL163, GLU168, THR304, VAL327, GLU323, GLU325, PHE328, ASN350,	-8.164	ASN23, ARG91, HIS125, LYS160, VAL16, GLY16, PHE32, GLU329
1TX2	-9.83	ARG88, ILE142, TRP143, ASN167, PHE209, ALA210, PRO213, ASN216, SER241	-10.922	VAL48, PRO50, GLY84, GLU85, SER86, ARG88, PHE91, VAL94, ARG102, LYS240, ARG274, HIS276	-12.031	PRO50, GLY84, GLU85, SER86, ARG88, PHE91, VAL94, ARG102, PHE209	-12.543	PRO50, GLY84, SER86, ARG88, PHE91, VAL94, GLU96, ARG102, PHE209, LYS240, ARG274, HIS276	-5.882	ARG88, LYS240, SER241, ARG254

Protein ID	Compound 134		Compound 143		Compound 174		Compounds 176		Reference Compound/CCL	
	B.A.	Int. Res.	B.A.	Int. Res.	B.A.	Int. Res.	B.A.	Int. Res.	B.A.	Int. Res.
2MLM	-10.686	ARG101, VAL110, LEU111, GLU113, GLN120, THR122, ILE124, ARG139, ILE141, VAL143	-11.011	VAL106, LEU111, GLU113, THR122, ILE124, ARG139, ILE141	-10.739	LEU39, HIS62, VAL110 LEU111, ILE124, TYR129, TRP136, ARG139, ILE141	11.415	GLU48, ASN56, ALA60, GLU113, THR122, ILE124, ARG139	-7.778	GLU47, VAL11, GLU11, LYS117, ILE124, ARG13, ILE141
4WOP	-9.69	THR11, LYS15, THR16, LYS37 THR41, ALA73, ALA110, GLY111,	-10.552	GLY10, THR11, GLY12, THR16, THR41, MET72, ALA110, GLY111, GLY112, LEU113, LEU114	-10.867	THR11, GLY12, LYS15, THR16, THR41, ASP48, GLU52, PRO71, GLY111	-11.628	THR11, GLY12, LYS15, THR16, VAL17, THR41, ASP48, GLU52, PRO71, GLY111	-8.3	GLY12, VAL13, GLY14, LYS15, THR16, VAL17, LYS37, ALA11, GLY111

B.A.: Binding affinity in terms of best binding energy (Kcal/mol), Int. Res.: interacting residues of the respective proteins with ligand.

Table 4: Physicochemical parameters of select coumarin-1,2,3-triazole hybrids.

Compd	Formula	MW	RBs	HBA	HBD	TPSA	Log P	LVs	VVs	BS	LLV	SA
134	$C_{27}H_{19}N_3O_5$	465.46	5	7	0	100.36	3.94	0	0	0.55	1	3.73
143	$C_{36}H_{32}N_6O_6$	644.68	10	10	0	140.3	4.9	2	1	0.17	3	4.78
174	$C_{33}H_{28}N_8O_6$	632.63	6	10	0	165.84	3.63	2	1	0.17	1	4.83
176	$C_{37}H_{24}N_8O_6$	676.64	6	10	0	165.84	3.87	3	1	0.17	2	4.79

MW: Molecular weight, RBs: No. of rotable bonds, HBA: Hydrogen bond acceptors, HBD: hydrogen bond donars, TPSA: Topilogical polar surface area, Log P: Consensus Log Po/w, LVs: No. of Lipinski violations, VVs: No. of Veber violations, BS: Bioavailability Score, LLV: No. of Lead likeness violations, SA: Synthetic Accessibility.

play a critical role in drug metabolism, as they are responsible for the biotransformation of the vast majority of drugs in the human body.[74,75] Understanding the role of Cytochrome P450 isoforms CYP1A2, CYP3A4, CYP2C9, CYP2C19, CYP2D6, and CYP2E1 in drug metabolism is crucial for predicting drug-drug interactions, determining drug efficacy, and assessing potential adverse effects.[67,76] Any compound that shows 50% inhibition at less than 10 μM is considered to be a CYP inhibitor. All the test compounds were non-inhibitors of CYP2D6 and non-substrates of CYP2D6. The excretion parameters discussed here are total clearance and renal OCT2 substrate.[45,67] The results obtained on the pkCSM server indicated that most of the compounds have higher total clearance and non-substrate renal OCT2. All the test compounds were non-sensitive to skin, but most of them had hepatotoxicity.

The famous Lipinski's rule of five for the drug-likeness of lead molecules sets the filtering criteria as hydrogen bond donors not greater than 5, hydrogen bond acceptors not greater than 10, molecular weight not greater than 500 Da, and octanol-water partition coefficient (log P) not greater than 5.[43] As straightforwardly stated, when a compound violates two or more of Lipinski's five rules, it is not considered to be active when taken orally.[43] Compound 134 showed zero violation of Lipinski's Rule of Five with a bioavailability score of 0.55 and a synthetic accessibility score of 3.73. The compounds 143 and 174 showed two violations, while compound 176 showed three violations to Lipinski. It has been observed that despite two or more Lipinski violations, many of the natural products and their derivatives have become successful oral drugs.[77,78] Actually, the natural cause of Lipinski violation is accompanied by high values for rotatable

Table 5: The score of various parameters for ADMET prediction of select coumarin-1,2,3-triazole hybrids.

Parameters		Compounds			
		134	143	174	176
Absorption	Caco2	0.342	0.176	0.565	0.392
	HIA	100	100	96.006	100
	SP	-2.735	-2.735	-2.735	-2.735
Distribution	VDss	0.103	-0.043	0.358	-0.059
	BBB	-1.146	-2.075	-2.315	-2.416
	CNS	-2.085	-3.691	-4.021	-3.938
Metabolism (CYPs inhibitor)	1A2	No	No	No	No
	2C19	Yes	Yes	Yes	Yes
	2C9	No	No	No	No
	2D6	Yes	No	No	No
	3A4	Yes	Yes	No	No
Excretion	TC	No	No	No	No
	OCT2	No	Yes	Yes	Yes
	AMES	1.226	-0.23	-0.58	1.724
Toxicity	ORAT	No	No	No	No
	ORCT	Yes	No	No	No
	HEP	Yes	Yes	Yes	Yes
	SS	No	No	No	No

Caco2: human colon epithelial cancer cell permeability, HIA: Human Intestinal absorption, SP: Skin Permeability, VDss: steady-state volume of distribution, BBB: Blood Brain Barrier permeability, CNS: Central Nervous System permeability, CYPs: cytochrome P450 isozymes (CYP1A2, CYP2C19, CYP2C9, CYP2D6, CYP3A4) inhibitors, TC: Total Clearance, OCT2: Renal OCT2 substrate, AMES: AMES Salmonella/microsome mutagenicity assay toxicity, ORAT: Oral Rat Acute Toxicity (LD50), ORCT: Oral Rat Chronic Toxicity (LOAEL), HEP: Hepatotoxicity, SS: Skin Sensitivity.

bonds, PSA, heavy atoms, and stereogenic centres.[77] The unique properties and therapeutic potential of natural products continue to make them valuable sources of drug discovery, highlighting the need to consider alternative guidelines when evaluating their drug-likeness. Hence, in merit of nature inspired lead, the molecules 143, 174, and 176 along with 134 were considered for MD simulation studies.

Molecular Dynamics

Considering the docking scores, physiochemical, and ADMET predictions, four compounds (134, 143, 174, and 176) were selected for MD simulation to test the stability with DNA Gyrase B24 (PDB: 6YD9) by using GROMACS. The simulation was run for 100 ns, and the results were analyzed on the basis of RMSD, RMSF, Radius of gyration, and hydrogen bond distribution. The radius of gyration helps to analyze the compactness of the atoms of proteins around its axis with respect to the time during the simulation. Figure 2 (a-d) shows the RMSD, RMSF, radius of gyration, and hydrogen bond distribution of 6YD9 with the selected four compounds 134**,** 143**,** 174, and 176. RMSD is a parameter to analyze the structural difference of proteins between conformations according to run time. The plot variation starts at 0.2 nm and is constant around 0.8 nm in compounds 143, but the plot varies up to 0.4 nm in the cases of compounds 134**,** 174, and 176**.** RMSD graphs clearly show that the most interactive residues of the active site of 6YD9 fluctuate more with compounds 143 and 143 but fluctuate least with compounds 174 and 176 (Figure 2b). So, compounds 134 and 143 may be omitted for further comparison on the basis of RMSD and RMSF analyses. The flattened graph of the radius of gyration, or minimal fluctuation graph, of 6YD9 with compounds shows the compactness of all complexes. Hydrogen bonds are responsible for stabilizing the protein-compound complex. Figure 2d shows hydrogen bonds during the 100 ns simulation. The hydrogen bond decreases in complexes of 6YD9 with 134**,** 143**,** and 174 over time as the simulation goes to 100 ns. The hydrogen bonds in 6YD9-174 increase up to 60ns, and then the number of hydrogen bonds decreases. But the complex of 6YD9-176 has a higher number of hydrogen bonds (3-5 H) throughout the simulation process, and 4-6 hydrogen bonds are formed in the last 20 ns.

Overall, MD simulation results are totally in agreement with the results of molecular docking. The graphical representation of the ligand-protein complexes revealed that the ligand conformations varied to a small extent during the simulation and were found to be well-fitted in the active site of the target proteins. Complex with 176 showed higher stability and interactions than the others.

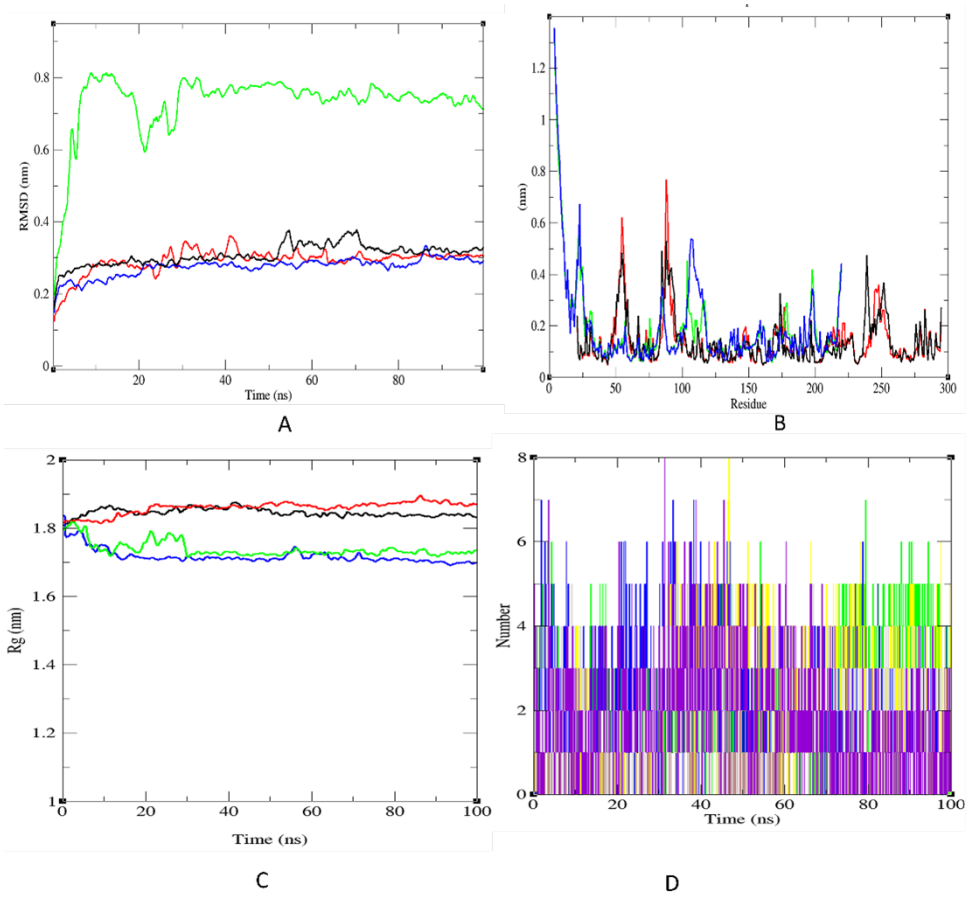

Figure 2: Representation graphs for Molecular dynamics simulation of selected four compounds 134, 143, 174 and 176 respectively A: RMSD, B: RMSF, C: Radius of gyration, D: Hydrogen bond number (in A, B, C: 143 (Green), 134 (Blue), 174 (Red), 176 (Black) and, in D: 143 (Blue), 134 (Yellow), 174 (Purple), 176 (Green).

CONCLUSION

The use of hybrid drug design in medicinal chemistry is an important technique for combining different substances to create bioactive substances that can be used to treat disease. In this work, computational approach for the exploration of 196 coumarin-1,2,3-triazole derivatives as potential antibacterial drug candidates were adopted. The high scores of ligand protein docking against three target proteins from Gram-positive and three from Gram-negative bacterial strains strengthened our approach for the development of multipotent ligands that can bind to more than one target. The compounds 176, 174, 175, and 145 showed almost double or even more binding energy than co-crystallized ligands, as did the antibiotic Dapsone against Gram-negative *E. coli* DNA Gyrase-B24 protein (6YD9). When focused on the ADMET and physicochemical properties of 70 compounds with high docking scores, many of them failed due to a greater number of violations in parameters for a drug candidate. Although compound 134 scored relatively poorly in docking studies, its pharmacokinetic properties are acceptable compared to other compounds, while 134, 143, 174, and 176 were considered for MD simulation because of high docking scores and in merit of nature inspired leads. Overall, 176 formed a stable complex with protein 6YD9 in MD simulation studies. We suggest detailed *in vitro* studies to explore the potential of hybrid molecules 134, 143, 174 and 176 as broad-spectrum antibacterial drug candidates.

ACKNOWLEDGEMENT

The authors thank the Director, Rajkiya Engineering College, Sonbhadra, for his constant encouragement and for providing all types of facilities for this study. We are thankful to Dr. Rajnish Kumar, Department of Pharmaceutical Engineering & Technology, Indian Institute of Technology (BHU), Varanasi-221005, for his help with the Molecular Dynamics simulation study.

AUTHORS' CONTRIBUTIONS

Krishna N. Mishra, Mayank Rashmi: Data collection, data curation, formal analysis, investigation, methodology, validation, visualization, drafting of manuscript. Harish C. Upadhyay: Conceptualization, data analysis, manuscript review and editing.

CONFLICT OF INTEREST

The authors declare no conflict of interest, financial or otherwise.

SUPPLEMENTARY MATERIAL

Grid centre coordinates and active site residues of selected six targets, docking scores of all the 196 coumarin-1,2,3-triazole hybrids in terms of binding energies of ligands with various antibacterial target proteins, and physicochemical and ADMET predictions of 70 coumarin-1,2,3-triazole hybrids (on the basis of high docking scores) are provided as supplementary material.

ABBREVIATIONS

CADD: Computer-Aided Drug Design; **FDA:** Food and Drug Administration; **PK:** pharmacokinetic; **PD:** Pharmacodynamics; **ADMET:** Absorption, Distribution, Metabolism, Excretion, and Toxicity; **HIV:** Human Immunodeficiency Viruses; **AMES:** *Salmonella typhimurium* reverse mutation assay (for toxicity assessment); **DNA:** Deoxyribonucleic acid; **RNA:** Ribonucleic acid; **RMSD:** Root Mean Square Deviation; **RMSF:** Root Mean Square Fluctuation.

SUMMARY

This research was carried out to investigate antibacterial potential of various coumarin-1,2,3-triazole hybrid molecules using CADD approach. Total 196 coumarin-1,2,3-triazole derivatives were screened for their binding affinities against three Gram-positive and three Gram-negative antibacterial target proteins through protein-ligand docking. Seventy compounds from the top 30 hits of all six target proteins in docking studies were evaluated for their physiochemical parameters on the SwissADME online tool, and pharmacokinetic parameters of ADMET on the pkCSM server. Further, on the basis of high docking score and suitable physiochemical and ADMET parameters, select hybrids were subjected to 100 ns of molecular dynamics (MD) on GROMACS to investigate the protein-ligand complex's stability and the results were analysed in terms of root mean square deviation (RMSD), root mean square fluctuation (RMSF), radius of gyration (Rg) and distribution of hydrogen bonds.

REFERENCES

1. Mohs RC, Greig NH. Drug discovery and development: role of basic biological research. Alzheimers Dement (N Y). 2017;3(4):651-7. doi: 10.1016/j.trci.2017.10.005, PMID 29255791.
2. Dickson M, Gagnon JP. The cost of new drug discovery and development. Discov Med. 2004;4(22):172-9. PMID 20704981.
3. Moscicki RA, Tandon PK. Drug-development challenges for small biopharmaceutical companies. N Engl J Med. 2017;376(5):469-74. doi: 10.1056/NEJMra1510070, PMID 28146666.
4. Mathur S, Hoskins C. Drug development: lessons from nature. Biomed Rep. 2017;6(6):612-4. doi: 10.3892/br.2017.909, PMID 28584631.
5. Hwang TJ, Carpenter D, Lauffenburger JC, Wang B, Franklin JM, Kesselheim AS. Failure of investigational drugs in late-stage clinical development and publication of trial results. JAMA Intern Med. 2016;176(12):1826-33. doi: 10.1001/jamainternmed.2016.6008, PMID 27723879.
6. Macalino SJY, Gosu V, Hong S, Choi S. Role of computer-aided drug design in modern drug discovery. Arch Pharm Res. 2015;38(9):1686-701. doi: 10.1007/s12272-015-0640-5, PMID 26208641.
7. Lee JW, Maria-Solano MA, Vu TNL, Yoon S, Choi S. Big data and artificial intelligence (AI) methodologies for computer-aided drug design (CADD). Biochem Soc Trans. 2022;50(1):241-52. doi: 10.1042/BST20211240, PMID 35076690.
8. Xiang M, Cao Y, Fan W, Chen L, Mo Y. Computer-aided drug design: lead discovery and optimization. Comb Chem High Throughput Screen. 2012;15(4):328-37. doi: 10.2174/138620712799361825, PMID 22221065.
9. Surabhi S, Singh B. Computer aided drug design: an overview. J Drug Deliv Ther. 2018;8(5):504-9. doi: 10.22270/jddt.v8i5.1894.
10. Kitchen DB, Decornez H, Furr JR, Bajorath J. Docking and scoring in virtual screening for drug discovery: methods and applications. Nat Rev Drug Discov. 2004;3(11):935-49. doi: 10.1038/nrd1549, PMID 15520816.
11. Lionta E, Spyrou G, Vassilatis DK, Cournia Z. Structure-based virtual screening for drug discovery: principles, applications and recent advances. Curr Top Med Chem. 2014;14(16):1923-38. doi: 10.2174/1568026614666140929124445, PMID 25262799.
12. Sliwoski G, Kothiwale S, Meiler J, Lowe EW. Computational methods in drug discovery. Pharmacol Rev. 2014;66(1):334-95. doi: 10.1124/pr.112.007336, PMID 24381236.
13. Lavecchia A, Cerchia C. *In silico* methods to address polypharmacology: current status, applications and future perspectives. Drug Discov Today. 2016;21(2):288-98. doi: 10.1016/j.drudis.2015.12.007, PMID 26743596.
14. Prieto-Martínez FD, López-López E, Eurídice Juárez-Mercado K, Medina-Franco JL. Computational drug design methods-current and future perspectives. In: *In silico* drug design: repurposing techniques and methodologies; 2019.
15. Upadhyay HC. Medicinal chemistry of alternative therapeutics: novelty and hopes with genus Ammannia. Curr Top Med Chem. 2019;19(10):784-94. doi: 10.2174/1568026619666190412101047, PMID 30977452.
16. Upadhyay HC. Exploring nature's treasure for drug discovery. Lett Drug Des Discov. 2023;20(4):373-4. doi: 10.2174/1570180820042301131444404.
17. Upadhyay HC, Singh M, Prakash O, Khan F, Srivastava SK, Bawankule DU. QSAR, ADME and docking guided semi-synthesis and *in vitro* evaluation of 4-hydroxy-α-tetralone analogs for anti-inflammatory activity. SN Appl Sci. 2020;2(12). doi: 10.1007/s42452-020-03798-5.
18. Saxena A, Upadhyay HC, Cheema HS, Srivastava SK, Darokar MP, Bawankule DU. Antimalarial activity of phytol derivatives: *in vitro* and *in vivo* study. Med Chem Res. 2018;27(5):1345-54. doi: 10.1007/s00044-017-2132-2.
19. GMC, DJ N. Natural products: A continuing source of novel drug leads. Biochim Biophys Acta (BBA) Gen Subj. 2013; 1830.
20. Newman DJ, Cragg GM. Natural products as sources of new drugs over the nearly four decades from 01/1981 to 09/2019. J Nat Prod. 2020;83(3):770-803. doi: 10.1021/acs.jnatprod.9b01285, PMID 32162523.
21. Upadhyay HC, Saini DC, Srivastava SK. Phytochemical analysis of Ammannia multiflora. Res J Phytochem. 2011;5(3).
22. Upadhyay HC, Thakur JP, Saikia D, Srivastava SK. Anti-tubercular agents from Ammannia baccifera (Linn.). Med Chem Res. 2013;22(1):16-21. doi: 10.1007/s00044-012-9998-9.
23. Stefanachi A, Leonetti F, Pisani L, Catto M, Carotti A. Coumarin: A natural, privileged and versatile scaffold for bioactive compounds. Molecules. 2018;23(2). doi: 10.3390/molecules23020250, PMID 29382051.
24. Matos MJ, Santana L, Uriarte E, Abreu OA, Molina E, Yordi EG. Coumarins-an important class of phytochemicals. In: Phytochemicals - isolation, characterisation and role in human health; 2015.
25. Akkol EK, Genç Y, Karpuz B, Sobarzo-Sánchez E, Capasso R. Coumarins and coumarin-related compounds in pharmacotherapy of cancer. Cancers. 2020;12.
26. Kumar S, Narasimhan B. Therapeutic potential of heterocyclic pyrimidine scaffolds. Chem Cent J. 2018;12(1):38. doi: 10.1186/s13065-018-0406-5, PMID 29619583.
27. Joule JA. Natural products containing nitrogen heterocycles-some highlights 1990-2015. Adv Heterocycl Chem. 2016;119:81-106. doi: 10.1016/bs.aihch.2015.10.005.
28. Guo HY, Chen ZA, Shen QK, Quan ZS. Application of triazoles in the structural modification of natural products. J Enzyme Inhib Med Chem. 2021;36(1):1115-44. doi: 10.1080/14756366.2021.1890066, PMID 34167422.
29. Jasovský D, Littmann J, Zorzet A, Cars O. Antimicrobial resistance-a threat to the world's sustainable development. Ups J Med Sci. 2016;121(3):159-64. doi: 10.1080/03009734.2016.1195900, PMID 27416324.
30. Zaman BS, Hussain MA, Nye R, Mehta V, Mamun KT, Hossain N. A review on antibiotic resistance: alarm bells are ringing. Cureus. 2017.
31. Murray CJ, Ikuta KS, Sharara F, Swetschinski L, Robles Aguilar G, Gray A. Global burden of bacterial antimicrobial resistance in 2019: a systematic analysis. Lancet. 2022;399(10325):629-55. doi: 10.1016/S0140-6736(21)02724-0, PMID 35065702.
32. Dwivedi GR, Upadhyay HC, Yadav DK, Singh V, Srivastava SK, Khan F, *et al.* 4-hydroxy-α-tetralone and its derivative as drug resistance reversal agents in multi drug resistant Escherichia coli. Chem Biol Drug Des. 2014;83(4):482-92. doi: 10.1111/cbdd.12263, PMID 24267788.
33. Spellberg B, Bartlett JG, Gilbert DN. The future of antibiotics and resistance. N Engl J Med. 2013;368(4):299-302. doi: 10.1056/NEJMp1215093, PMID 23343059.

34. Shaveta MS, Mishra S, Singh P. Hybrid molecules: the privileged scaffolds for various pharmaceuticals. Eur J Med Chem. 2016;124:500-36. doi: 10.1016/j.ejmech.2016.08.039, PMID 27598238.
35. Parkes AL, Yule IA. Hybrid antibiotics - clinical progress and novel designs. Expert Opin Drug Discov. 2016;11(7):665-80. doi: 10.1080/17460441.2016.1187597, PMID 27169483.
36. Meunier B. Hybrid molecules with a dual mode of action: dream or reality? Acc Chem Res. 2008;41(1):69-77. doi: 10.1021/ar7000843, PMID 17665872.
37. Mishra KN, Upadhyay HC. Coumarin-1,2,3-triazole hybrids as leading-edge anticancer agents. Front Drug Discov. 2022;2. doi: 10.3389/fddsv.2022.1072448.
38. Upadhyay HC. Coumarin-1,2,3-triazole hybrid molecules: an emerging scaffold for combating drug resistance. Curr Top Med Chem. 2021;21(8):737-52. doi: 10.2174/1568026621666210303145759, PMID 33655863.
39. Morris GM, Huey R, Lindstrom W, Sanner MF, Belew RK, Goodsell DS *et al.* AutoDock4 and AutoDockTools4: automated docking with selective receptor flexibility. J Comput Chem. 2009;30(16):2785-91. doi: 10.1002/jcc.21256, PMID 19399780.
40. Eberhardt J, Santos-Martins D, Tillack AF, Forli, AutoDock V. New. AutoDock Vina 1.2.0: New Docking Methods, Expanded Force Field, and Python Bindings. J Chem Inf Model. 2021;61(8):3891-8. doi: 10.1021/acs.jcim.1c00203, PMID 34278794.
41. Trott O, Olson AJ. AutoDock Vina: improving the speed and accuracy of docking with a new scoring function, efficient optimization, and multithreading. J Comput Chem. 2010;31(2):455-61. doi: 10.1002/jcc.21334, PMID 19499576.
42. Daina A, Michielin O, Zoete V. SwissADME: A free web tool to evaluate pharmacokinetics, drug-likeness and medicinal chemistry friendliness of small molecules. Sci Rep. 2017;7:42717. doi: 10.1038/srep42717, PMID 28256516.
43. Lipinski CA, Lombardo F, Dominy BW, Feeney PJ. Experimental and computational approaches to estimate solubility and permeability in drug discovery and development settings. Adv Drug Deliv Rev. 2012;64.
44. Benet LZ, Hosey CM, Ursu O, Oprea TI. BDDCS, the Rule of 5 and drugability. Adv Drug Deliv Rev. 2016;101:89-98. doi: 10.1016/j.addr.2016.05.007, PMID 27182629.
45. Pires DEV, Blundell TL, Ascher DB. pkCSM: Predicting small-molecule pharmacokinetic and toxicity properties using graph-based signatures. J Med Chem. 2015;58(9):4066-72. doi: 10.1021/acs.jmedchem.5b00104, PMID 25860834.
46. Abraham MJ, Murtola T, Schulz R, Páll S, Smith JC, Hess B, *et al.* Gromacs: high performance molecular simulations through multi-level parallelism from laptops to supercomputers. SoftwareX. 2015; 1-2: 19-25. doi: 10.1016/j.softx.2015.06.001.
47. Huang J, Rauscher S, Nawrocki G, Ran T, Feig M, De Groot BL, *et al.* CHARMM36m: an improved force field for folded and intrinsically disordered proteins. Nat Methods. 2017;14(1):71-3. doi: 10.1038/nmeth.4067, PMID 27819658.
48. Jo S, Kim T, Iyer VG, Im W, CHARMM-GUI, CHARMM-GUI. CHARMM-GUI: A web-based graphical user interface for CHARMM. J Comput Chem. 2008;29(11):1859-65. doi: 10.1002/jcc.20945, PMID 18351591.
49. Morozova TI, García NA, Barrat JL. Temperature dependence of thermodynamic, dynamical, and dielectric properties of water models. J Chem Phys. 2022;156(12):126101. doi: 10.1063/5.0079003, PMID 35364874.
50. Jo S, Kim T, Im W. Automated builder and database of protein/membrane complexes for molecular dynamics simulations. PLOS ONE. 2007;2(9):e880. doi: 10.1371/journal.pone.0000880, PMID 17849009.
51. Hess B, Bekker H, Berendsen HJC, Fraaije JGEM. Lincs: A Linear Constraint Solver for molecular simulations. J Comput Chem. 1997;18(12):1463-72. doi: 10.1002/(SICI)1096-987X(199709)18: 12<1463::AID-JCC4>3.0.CO;2-H.
52. Basconi JE, Shirts MR. Effects of temperature control algorithms on transport properties and kinetics in molecular dynamics simulations. J Chem Theor Comput. 2013;9(7):2887-99. doi: 10.1021/ct400109a, PMID 26583973.
53. Martoňák R, Laio A, Parrinello M. Predicting crystal structures: the Parrinello-Rahman method revisited. Phys Rev Lett. 2003;90(7):075503. doi: 10.1103/PhysRevLett.90.075503, PMID 12633242.
54. Kohanski MA, Dwyer DJ, Collins JJ. How antibiotics kill bacteria: from targets to networks. Nat Rev Microbiol. 2010;8(6):423-35. doi: 10.1038/nrmicro2333, PMID 20440275.
55. Sainsbury S, Bird L, Rao V, Shepherd SM, Stuart DI, Hunter WN, *et al.* Crystal structures of penicillin-binding protein 3 from pseudomonas aeruginosa: comparison of native and antibiotic-bound forms. J Mol Biol. 2011;405(1):173-84. doi: 10.1016/j.jmb.2010.10.024, PMID 20974151.
56. Skok Ž, Barančoková M, Benek O, Cruz CD, Tammela P, Tomašič T, *et al.* Exploring the chemical space of benzothiazole-based DNA gyrase B inhibitors. ACS Med Chem Lett. 2020;11(12):2433-40. doi: 10.1021/acsmedchemlett.0c00416, PMID 33329764.
57. Skarzynski T, Mistry A, Wonacott A, Hutchinson SE, Kelly VA, Duncan K. Structure of UDP-N-acetylglucosamine enolpyruvyl transferase, an enzyme essential for the synthesis of bacterial peptidoglycan, complexed with substrate UDP-N-acetylglucosamine and the drug fosfomycin. Structure. 1996;4(12):1465-74. doi: 10.1016/s0969-2126(96)00153-0, PMID 8994972.
58. Babaoglu K, Qi J, Lee RE, White SW. Crystal structure of 7,8-dihydropteroate synthase from Bacillus anthracis: mechanism and novel inhibitor design. Structure. 2004;12(9):1705-17. doi: 10.1016/j.str.2004.07.011, PMID 15341734.
59. Zhulenkovs D, Rudevica Z, Jaudzems K, Turks M, Leonchiks A. Discovery and structure-activity relationship studies of irreversible benzisothiazolinone-based inhibitors against Staphylococcus aureus sortase A transpeptidase. Bioorg Med Chem. 2014;22(21):5988-6003. doi: 10.1016/j.bmc.2014.09.011, PMID 25282649.
60. Salaemae W, Yap MY, Wegener KL, Booker GW, Wilce MCJ, Polyak SW. Nucleotide triphosphate promiscuity in Mycobacterium tuberculosis dethiobiotin synthetase. Tuberculosis (Edinb). 2015;95(3):259-66. doi: 10.1016/j.tube.2015.02.046, PMID 25801336.
61. Lohani S, Cooper H, Jin X, Nissley BP, Manser K, Rakes LH, *et al.* Physicochemical properties, form, and formulation selection strategy for a biopharmaceutical classification system class II preclinical drug candidate. J Pharm Sci. 2014;103(10):3007-21. doi: 10.1002/jps.24088, PMID 25074668.
62. Durán-Iturbide NA, Díaz-Eufracio BI, Medina-Franco JL. *In silico* ADME/Tox profiling of natural products: A focus on BIOFACQUIM. ACS Omega. 2020;5(26):16076-84. doi: 10.1021/acsomega.0c01581, PMID 32656429.
63. Sun D, Gao W, Hu H, Zhou S. Why 90% of clinical drug development fails and how to improve it? Acta Pharm Sin B. 2022;12(7):3049-62. doi: 10.1016/j.apsb.2022.02.002, PMID 35865092.
64. Meanwell NA. Improving drug candidates by design: A focus on physicochemical properties as a means of improving compound disposition and safety. Chem Res Toxicol. 2011;24(9):1420-56. doi: 10.1021/tx200211v, PMID 21790149.
65. Mvondo JGM, Matondo A, Mawete DT, Bambi SN, Mbala BM, Lohohola PO. *In silico* ADME/T properties of quinine derivatives using SwissADME and pkCSM webservers. Int J Trop Dis Health. 2021:1-12. doi: 10.9734/ijtdh/2021/v42i1130492.
66. Masaoka Y, Tanaka Y, Kataoka M, Sakuma S, Yamashita S. Site of drug absorption after oral administration: assessment of membrane permeability and luminal concentration of drugs in each segment of gastrointestinal tract. Eur J Pharm Sci. 2006; 29(3-4):(3-4)(3-4 SPEC. ISS.). doi: 10.1016/j.ejps.2006.06.004, PMID 16876987.
67. Biharee A, Yadav A, Jangid K, Singh Y, Kulkarni S, Sawant DM, *et al.* Flavonoids as promising anticancer agents: an *in silico* investigation of ADMET, binding affinity by molecular docking and molecular dynamics simulations. J Biomol Struct Dyn. 2023;41(16):7835-46. doi: 10.1080/07391102.2022.2126397, PMID 36165610.
68. Paudel KS, Milewski M, Swadley CL, Brogden NK, Ghosh P, Stinchcomb AL. Challenges and opportunities in dermal/transdermal delivery. Ther Deliv. 2010;1(1):109-31. doi: 10.4155/tde.10.16, PMID 21132122.
69. Lin J, Sahakian DC, de Morais SM, Xu JJ, Polzer RJ, Winter SM. The role of absorption, distribution, metabolism, excretion and toxicity in drug discovery. Curr Top Med Chem. 2003;3(10):1125-54. doi: 10.2174/1568026033452096, PMID 12769713.
70. Yamashita S, Furubayashi T, Kataoka M, Sakane T, Sezaki H, Tokuda H. Optimized conditions for prediction of intestinal drug permeability using Caco-2 cells. Eur J Pharm Sci. 2000;10(3):195-204. doi: 10.1016/s0928-0987(00)00076-2, PMID 10767597.
71. Cecchelli R, Berezowski V, Lundquist S, Culot M, Renftel M, Dehouck MP, *et al.* Modelling of the blood-brain barrier in drug discovery and development. Nat Rev Drug Discov. 2007;6(8):650-61. doi: 10.1038/nrd2368, PMID 17667956.
72. Koziara JM, Lockman PR, Allen DD, Mumper RJ. In situ blood-brain barrier transport of nanoparticles. Pharm Res. 2003;20(11):1772-8. doi: 10.1023/b:pham.0000003374.58641.62, PMID 14661921.
73. Niazi S. Volume of distribution as a function of time. J Pharm Sci. 1976;65(3):452-4. doi: 10.1002/jps.2600650339, PMID 1263103.
74. Zhao M, Ma J, Li M, Zhang Y, Jiang B, Zhao X, *et al.* Cytochrome P450 enzymes and drug metabolism in humans. Int J Mol Sci. 2021;22(23). doi: 10.3390/ijms222312808, PMID 34884615.
75. Zanger UM, Schwab M. Cytochrome P450 enzymes in drug metabolism: regulation of gene expression, enzyme activities, and impact of genetic variation. Pharmacol Ther. 2013;138(1):103-41. doi: 10.1016/j.pharmthera.2012.12.007, PMID 23333322.
76. Leow JWH, Chan ECY. Atypical Michaelis-Menten kinetics in cytochrome P450 enzymes: A focus on substrate inhibition. Biochem Pharmacol. 2019;169:113615. doi: 10.1016/j.bcp.2019.08.017, PMID 31445022.
77. Ganesan A. The impact of natural products upon modern drug discovery. Curr Opin Chem Biol. 2008;12(3):306-17. doi: 10.1016/j.cbpa.2008.03.016, PMID 18423384.
78. Benet LZ, Broccatelli F, Oprea TI. BDDCS applied to over 900 drugs. AAPS J. 2011;13(4):519-47. doi: 10.1208/s12248-011-9290-9, PMID 21818695.

Cite this article: Mishra KN, Rashmi M, Upadhyay HC. Coumarin-1,2,3-Triazole Hybrids as Promising Antibacterial Agents: *In silico* Molecular Docking, ADMET and Molecular Dynamics Simulation Studies (Exploring in silico Antibacterial Potential of Coumarin-1,2,3-triazoles). Indian J of Pharmaceutical Education and Research. 2024;58(4):1242-54.